ACCOUNTS
of chemical research

Photochemistry of the Water Molecule: Adiabatic versus Nonadiabatic Dynamics

KAIJUN YUAN,[†] RICHARD N. DIXON,[‡] AND XUEMING YANG*,[†]

[†]*State Key Laboratory of Molecular Reaction Dynamics, Dalian Institute of Chemical Physics, Chinese Academy of Sciences, Dalian, China, and* [‡]*School of Chemistry,University of Bristol, Bristol BS8 1TS, United Kingdom*

RECEIVED ON DECEMBER 1, 2010

CONSPECTUS

Water and light are two common constituents of both the earth's atmosphere and interstellar space. Consequently, water photodissociation is a central component of the chemistry of these environments. Electronically excited molecules can dissociate adiabatically (on a single potential energy surface, or PES) or nonadiabatically (with transfer between PESs), and water serves as a prototype for understanding these two processes in unimolecular dissociation. In recent years, extensive experimental and theoretical studies have been focused on water photolysis, particularly on the primary product of the dissociation, the OH radical. The use of the high-resolution H-atom Rydberg tagging technique, in combination with various vacuum ultraviolet (VUV) sources, has spurred significant advances in water photochemistry. As the excitation energy increases, different excited electronic states of water can be reached, and the mutual interactions between these states increase significantly. In this Account, we present the most recent developments in water photodissociation that have been derived from the study of the four lowest electronic excited states.

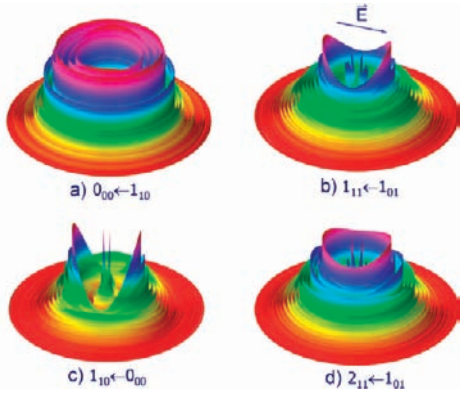

The $\tilde{A}^1B_1$ state photodissociation of H_2O has been studied at 157.6 nm and was found to be a fast and direct dissociation process on a single repulsive surface, with only vibrational excitation of the OH($X^2\Pi$) product. In contrast, the dissociation of the $\tilde{B}^1A_1$ state was found to proceed via two main routes: one adiabatic pathway leading to OH($A^2\Sigma^+$) + H, and one nonadiabatic pathway to OH($X^2\Pi$) + H through conical intersections between the $\tilde{B}$ state and the ground state $\tilde{X}^1A_1$. An interesting quantum interference between two conical intersection pathways has also been observed. In addition, photodissociation of H_2O between 128 and 133 nm has been studied with tunable VUV radiation. Experimental results illustrate that excitation to the different unstable resonances of the state has very different effects on the OH($X^2\Pi$) and OH($A^2\Sigma^+$) product channels.

The $\tilde{C}^1B_1$ state of H_2O is a predissociative Rydberg state with fully resolved rotational structures. A striking variation in the OH product state distribution and its stereodynamics has been observed for different rotational states. There are two kinds of nonadiabatic dissociation routes on the $\tilde{C}$ state. The first involves Renner−Teller (electronic Coriolis) coupling to the $\tilde{B}$ state, leading to rotationally hot and vibrationally cold OH products. The second goes through a newly discovered homogeneous nonadiabatic coupling to the $\tilde{A}$ state, leading to rotationally cold and vibrationally hot OH products. But the $\tilde{D}^1A_1$ state shows no rotational structure and leads to a fast, homogeneous, purely electronic predissociation to the $\tilde{B}$ state.

These studies demonstrate the truly fascinating nature of water photochemistry, which is extremely variable because of the different electronic states and their interactions. The results also provide a rather complete picture of water photochemistry and should be helpful in the modeling of interstellar chemistry, with its abundant VUV radiation.

I. Introduction

Molecular photodissociation has long been viewed as an interesting and challenging area of chemical physics, the results of which are essential to our understanding of important processes in vision chemistry,[1] atmospheric chemistry, and interstellar chemistry.[2] Adiabatic dissociation (occurring on the single potential energy surface (PES)) and nonadiabatic dissociation (transferring from one PES to another) processes may occur when a molecule is electronically excited. The H_2O molecule is one of the most

Published on the Web 03/23/2011 www.pubs.acs.org/accounts
10.1021/ar100153g

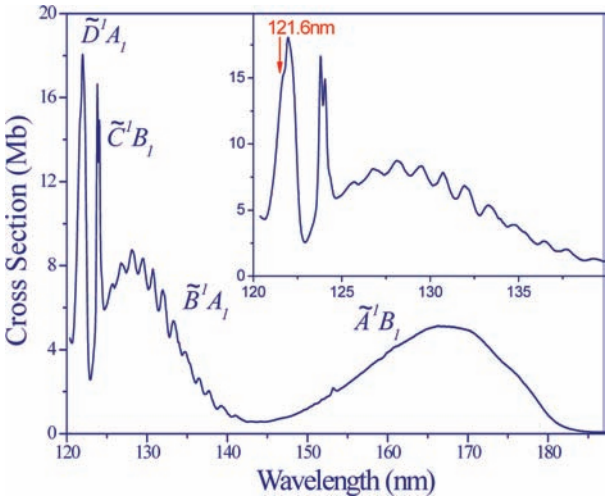

FIGURE 1. Absorption spectrum of H_2O at room temperature (1 Mb = 1×10^{-18} cm^2). The lowest four electronic states of H_2O have been observed.

prototypical systems for unimolecular dissociation studies. It has served as a model system for the understanding of adiabatic and nonadiabatic dissociation processes. The first four excited electronic states of water are considered to be of mixed Rydberg−valence character, each showing their own distinctive photochemistry.

The ground state water molecule has C_{2v} symmetry, and the electronic configuration is $(1a_1)^2(2a_1)^2(3a_1)^2(1b_1)^2$; $\tilde{X}^1A_1$. It has rich electronic absorption bands in the vacuum ultraviolet (VUV) region below 200 nm (Figure 1)[3] induced by excitations of one electron from the $1b_1$ or $3a_1$ orbital to higher orbitals. The water photochemistry has been studied at many different wavelengths. Excitation in its longest wavelength ultraviolet absorption band around 150−200 nm leads to the lowest excited singlet state ($\tilde{A}^1B_1$), which arises as a result of electron promotion from the $1b_1$ molecular orbital to an antibonding orbital with a_1 symmetry. Dissociation on this state is a rare prototype of direct dissociation processes that can be studied from first principles. During the last decade or so, photodissociation of H_2O from the $\tilde{A}$ state has been extensively studied both theoretically[4−7] and experimentally.[8−13] Good agreements have been found between theory and experiment in the rotational distributions of the OH(v) product from H_2O photodissociation at 157 nm. However, there are significant discrepancies between the calculated[14,15] and experimental[16,17] vibrational state distributions of the OH products.

The second absorption band, centered around 128 nm, shows some diffuse structures with a spacing of ~810 cm^{-1}. This absorption is assigned to the $\tilde{B}^1A_1 \leftarrow \tilde{X}^1A_1$ transition, arising as a result of electron promotion from the in-plane nonbonding $3a_1$ orbital to the $3sa_1$ Rydberg orbital. The diffuse progression of bands has been interpreted as unstable periodic orbits involving a combination of bending and HO−H stretching motion.[18−21] Dissociation on the $\tilde{B}$ state has been investigated at the Lyman-α wavelength (121.6 nm),[22−24] which exhibits much more complicated and interesting dynamics largely due to the conical intersection between the $\tilde{B}$ and $\tilde{X}$ surfaces. Coupling between $\tilde{B}$ and $\tilde{A}$ states is also possible near the linear geometry of the H_2O molecule because these two states are degenerate components of a $^1\Pi_u$ state at the linear geometry. Adiabatic dissociation on the $\tilde{B}$ surface leads to an H atom and an electronically excited OH($A^2\Sigma^+$) radical. This process is relatively minor in comparison with the dominant dissociation process that produces an H atom plus the electronically ground state OH ($X^2\Pi$) via nonadiabatic transition from the $\tilde{B}$ state to the $\tilde{A}$ state or the ground state of water ($\tilde{X}^1A_1$).[25,26] Photodissociation of water in the deep VUV region has also been studied using tunable synchrotron radiation.[27,28]

Conical intersections between PESs have been recognized as playing an important role in the dynamics of excited electronic state photochemistry: the H_2O $\tilde{B}$ state is a well-known example. One of the notable observations from experimental studies is the extremely high rotational excitation of the OH product. This is attributed to a conical intersection at a collinear (H−O−H) geometry. This conical intersection arises because a linear approach of H to OH on the repulsive potential curve from H + OH($X^2\Pi$) can cross an attractive potential curve from H + OH($A^2\Sigma^+$), whereas there is an avoided crossing of these curves in the lower symmetry of a bent geometry. In addition to the conical intersection for the H−O−H geometry, there is a second symmetry-determined conical intersection on the $\tilde{B}$ state for the collinear O−H−H geometry. The importance of this second conical intersection in the O(^{1}D, ^{3}P) + H_2 reaction system has been illustrated before.[29] However, only recently has its possible influence on the H_2O photochemistry been seriously addressed. Mordaunt et al.[30] pointed out, in a recent wavepacket calculation, that a small part of the dissociative flux on the $\tilde{B}$ surface goes toward the second conical intersection (O−H−H), thus indicating that this second intersection might also play a role in the $\tilde{B}$ state photodissociation and cause quantum interference.

The $\tilde{C}^1B_1 \leftarrow \tilde{X}^1A_1$ band of H_2O is located around 124 nm. Electronic structure calculations reveal that the $\tilde{C}$ state wave function is dominated by the 3p Rydberg configuration $(1b_1)^1(3pa_1)^1$ in the vertical Franck−Condon region. From spectroscopic studies, the $\tilde{C}$ state was found to be

predissociative with a lifetime of a few picoseconds. In addition, the predissociation lifetime is clearly rotational dependent, suggesting that more than one predissociation mechanism is associated with this electronic state. Rotationally excited OH(A) products were observed through the spontaneous A → X fluorescence after the excitation of the $\tilde{C}$ state.[31−34] The next electronic state is the $\tilde{D}^1A_1$ state with the electron promotion from the $1b_1$ orbital to the 3p Ryberg b_1 orbital. The absorption spectrum of the $\tilde{D}$ state is around 120 nm and shows no rotational structure because of the extremely strong coupling to the $\tilde{B}$ state at bent geometry (strong interaction between the $(1a_1)^2(2a_1)^2(3a_1)^1(1b_1)^2(3sa_1)^1$ and $(1a_1)^2(2a_1)^2(3a_1)^2(1b_1)^1(3pb_1)^1$ configurations).[35]

In the last decade, we have investigated systematically the photochemistry of water through the $\tilde{A}$, $\tilde{B}$, $\tilde{C}$, and $\tilde{D}$ states by using the high-resolution H-atom Rydberg tagging technique in combination with various VUV light sources. These results have provided a uniquely clear picture of water photochemistry in nearly the entire VUV region at the fully quantum state-to-state level.

II. Experimental Approaches

The H-atom Rydberg tagging time-of-flight technique (HRTOF) was developed in the early 1990s by Welge and co-workers.[36] The central scheme of this technique is the two-step efficient excitation of the H atom from its ground state to high Rydberg levels ($n = 35-90$) without ionizing the H-atom product. These neutral H atoms allow us to measure the TOF spectrum of the H-atom product with extremely high translational energy (TE) resolution: as high as 0.1% resolution in TE has been achieved. The 121.6 nm VUV light used in the first step excitation is generated using a two-photon resonant difference ($2\omega_1 - \omega_2$) four-wave mixing (DFWM) scheme in the Kr gas cell, with $\lambda_1 = 212.5$ nm and $\lambda_2 = 845$ nm. Following the first step excitation, the H-atom product is then sequentially excited to a high Rydberg state using 365 nm light in near saturation. The neutral Rydberg H atoms then fly a certain TOF distance to reach an MCP detector with a fine metal grid in the front. After passing through the grid, the Rydberg H-atom products are immediately field-ionized by the electric field applied between the front plate of the Z-stack MCP detector and the fine metal grid.

In the H_2O photodissociation experiments, dissociation dynamics at different photolysis wavelengths were studied. The experimental apparatus used for the H_2O photodissociation study has been described in ref 43. In addition to the 157 and 121.6 nm used for photolysis, we have also used a tunable VUV source for the photolysis source. The tunable VUV light is generated using DFWM of the same λ_1 (212.5 nm) light for generating 121.6 nm light used for the first step of the H-atom Rydberg tagging and another tunable source from 532 to 750 nm.[37] A molecular beam of H_2O was generated by expanding a mixture of H_2O/Ar through a pulsed nozzle. The rotational temperature of the H_2O molecules in the molecular beam is around 10 K.[38] The detector in the photodissociation experiment is fixed in a direction perpendicular to that of the molecular beam. The molecular beam and the photolysis laser beam are perpendicular to each other.

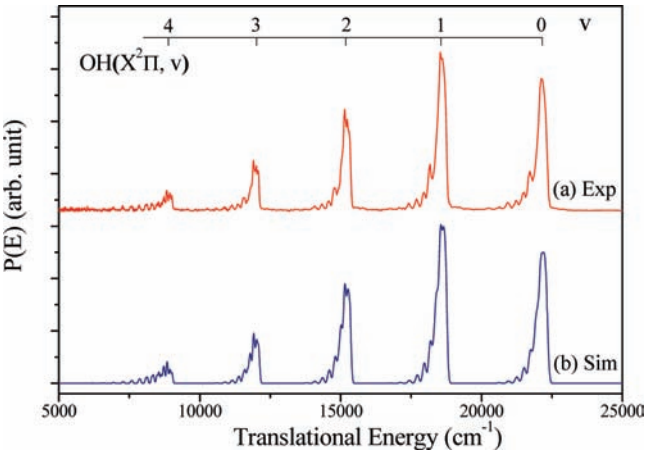

FIGURE 2. The experimental and simulated product translational energy distribution in the center-of-mass frame for H_2O photodissociation at 157 nm.

III. H_2O Photochemistry via the $\tilde{A}^1B_1$ Surface: Direct Dissociation

Photodissociation of H_2O on the $\tilde{A}^1B_1$ surface has been studied at 157.6 nm using the HRTOF technique.[39−41] The TOF spectrum of the H-atom product from H_2O photodissociation was measured and then converted into the product translational energy spectrum. Figure 2 shows the product TE spectrum of H_2O photodissociation at 157.6 nm with a molecular beam. Five vibrational features have been observed in the spectrum, which can be assigned to the vibrational excited OH($\nu = 0$, 1, 2, 3, 4) products. Rotational structures with higher rotational quantum number are partially resolved. By simulating and integrating each individual peak in the TE spectrum, the OH product vibrational distributions for the molecular beam and the water vapor can be obtained (Figure 3). Experimental results by the laser-induced fluorescence (LIF) method and theoretical results are also shown for comparison. By comparison of the cold molecular beam result with the room temperature vapor result, it seems that the rotational excitation of the parent

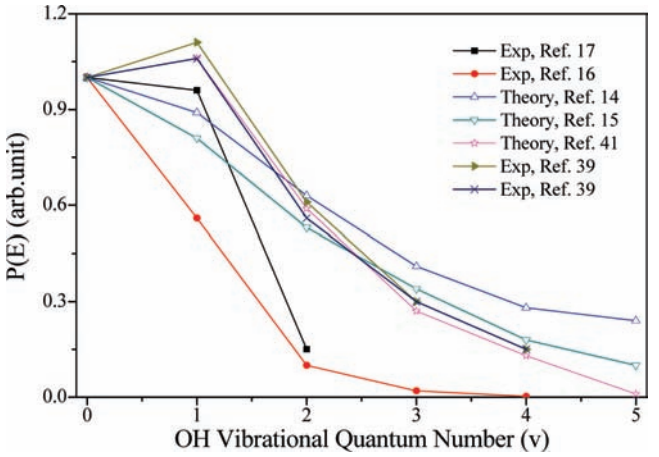

FIGURE 3. Comparison of the vibrational state distributions of the OH product obtained from theoretical and experimental studies for H_2O photodissociation at 157 nm.

molecule has a negligible effect on the OH product vibrational distribution from H_2O photodissociation at 157.6 nm..

The OH product vibrational distributions obtained by HRTOF are significantly different from the one measured using the LIF method,[16,17] especially for the higher vibrational states. This indicates that the vibrational distribution of OH obtained by previous LIF measurements may have serious errors. There are a few problems involved when one uses LIF to measure relative OH product vibrational populations. For example, propagation errors caused by changing laser dyes to cover all vibrational states, the errors caused by saturation effects, and the inaccurate off-diagonal Franck−Condon factors used in calibrating the LIF intensities. Predissociation of OH in the excited electronic state in the LIF scheme can also cause serious errors.

From Figure 3, the vibrational state distributions of the OH product obtained under the two experimental conditions are in good agreement with the theoretical results,[14,15] suggesting that the overall accuracy of the theoretical calculations are fairly good for the $v \leq 4$ levels. There is, however, a large discrepancy between the previous theoretical results and experimental measurement at $v = 5$. This could come from the inaccuracies of the H_2O $\tilde{A}$ state PES on which all previous theoretical calculations are based. Recent theoretical studies[42] based on an improved PES have shown that this is truly the case. The agreement between the product state distributions from theory and experiment is much improved for H_2O. This improved $\tilde{A}$ state PES is now believed to be one of the most accurate model potentials for direct dissociation processes in triatomic molecules.

Photodissociation of D_2O via the $\tilde{A}$ state at 157.6 nm has also been investigated. Seven vibrational features have been

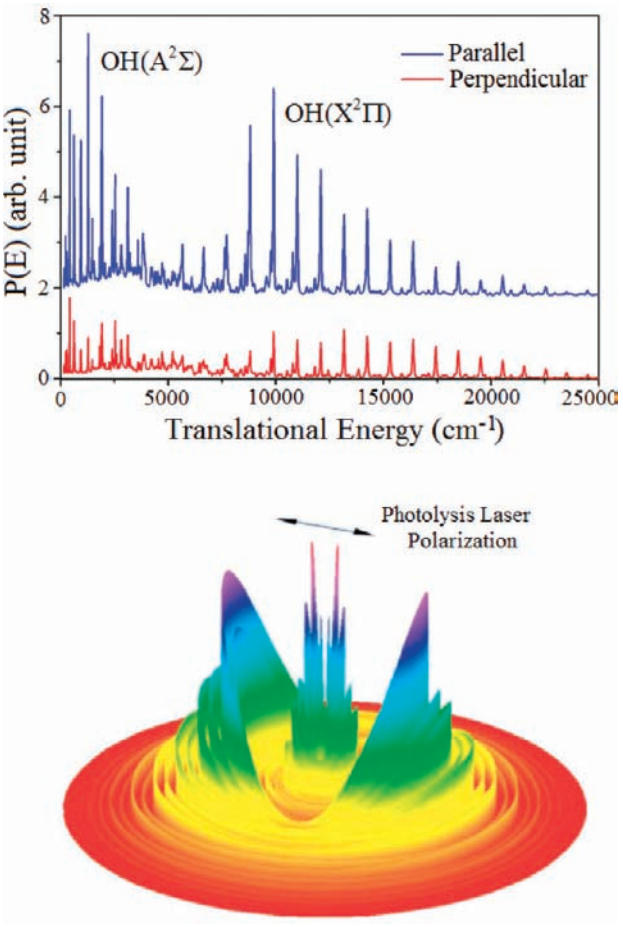

FIGURE 4. (upper panel) The total translational energy distributions of the photofragments from photodissociation at 121.6 nm of H_2O in a cold molecular beam with laser polarization parallel and perpendicular to the detection axis. (lower panel) The 3D contour of the product translational energy distribution: the inside feature of peaks is due to the OH $A^2\Sigma^+$ and the outer group to its ground $X^2\Pi$ state.

observed. These features can be assigned to the vibrational excited OD products with $v = 0-6$. Because of the smaller OD rotational constant, the rotational structures are not as well resolved as in the H_2O case. It is interesting to point out that even though more vibrational states of the OD product in the D_2O photodissociation are populated in comparison with the OH product from H_2O photodissociation, the vibrational energy deposited into the OD product is quite similar to the OH product. The averaged vibrational energy deposited in the OH product is about 4170 cm^{-1}, while that deposited in the OD product is about 4310 cm^{-1}.

IV. H_2O photochemistry via the $\tilde{B}^1A_1$ Surface: Dissociation through Conical Intersections

Dissociation of H_2O on the $\tilde{B}^1A_1$ surface is a much more complicated case than on the $\tilde{A}$ surface.[43] Three electronic

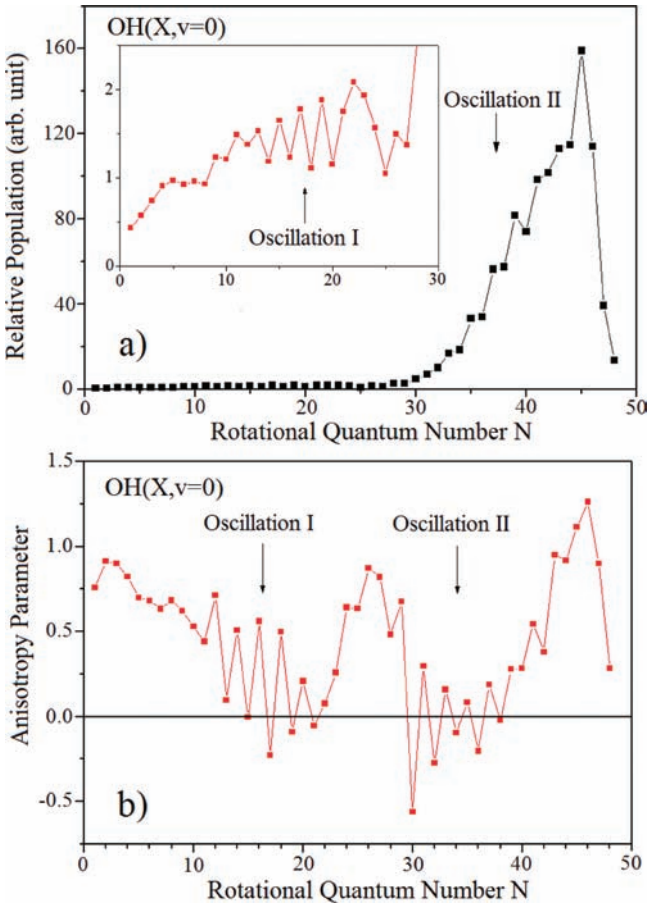

FIGURE 5. (a) The rotational state distribution of the OH(X, $\nu = 0$) product from H_2O photodissociation at 121.6 nm. (b) Rotational state dependence of the anisotropy parameter β for the OH(X, $\nu = 0$) product. There are two local ranges of oscillation in the distributions: one is at $N \approx 16$, and the other is at $N \approx 34$.

states have been implicated in the photochemistry of H_2O at 121.6 nm. Figure 4 shows the TE distribution of the products from H_2O photodissociation at 121.6 nm using two different laser polarization schemes. The three-dimensional (3D) contour of the TE distribution has also been shown in Figure 4. It is obvious that the most important pathway leads to the OH ground electronic state products in the $\nu = 0$ state. Figure 5a shows the rotational distributions of the OH(X, $\nu = 0$) product obtained from the simulations. Most of the OH(X, $\nu = 0$) products are extremely rotationally excited with a peak at $N = 45$, corresponding to about 32 000 cm^{-1} rotational excitation. This is truly a phenomenal case in that almost 75% of the available energy is deposited into purely rotational excitation. Dynamical calculation using time-dependent wavepackets[30] have shown that the high average rotational angular momentum of the OH product is the consequence of a high torque acting in the vicinity of the conical intersection at a collinear (H−O−H) geometry between $\tilde{B}$ and $\tilde{X}$ surfaces.

The most interesting observation in 121.6 nm photodissociation of H_2O is the intensity oscillations of the OH(X, $\nu = 0$) rotational distribution. Figure 5a shows a clear oscillation around $N = 40$, with the odd N levels having enhanced population with respect to the neighboring even N levels. There is also another oscillation in the weaker peaks of the rotational distribution near $N = 16$. The two oscillations have also been observed in exactly the same region of the distribution for the rotational-dependent angular anisotropy parameter (Figure 5b). Two-dimensional quantum dynamical calculations,[44] which span the regions that include both H−O−H and O−H−H conical intersections between the $\tilde{B}$ and $\tilde{X}$ surfaces, show that the even/odd intensity alternation in the OH($\nu = 0$) rotational distribution arises through a quantum interference between components of the wave function emanating on the $\tilde{X}$ surface from these two conical intersections. The recent 3D dynamical calculations by Dixon[22] also show the quantum interference between waves emanating from the two dissimilar conical intersections on the $\tilde{X}$ surface. The interference pattern and the OH product rotational distribution are sensitive to the positions and energies of the conical intersections. This interesting feature provides a chemical analog of Young's well-known double-slit experiment.

The substitution of a hydrogen atom in H_2O by one deuterium atom often leads to significant changes in dynamics, particularly where nonadiabatic dissociation is involved. An HOD photodissociation experiment has recently been carried out to investigate such a dynamical effect.[45] The observed highest peak in the product TE spectrum below the dissociation limit is the $N = 47$ level of OH($X^2\Pi$, $\nu = 0$), which has a rotational energy of 33 400 cm^{-1}, already 94% of the bond dissociation energy of the OH molecule. Even more interesting, OH rotational states ($N = 49$, 50) above its dissociation limit have been detected. These extremely rotationally excited levels are clearly quasibound through the support of a centrifugal barrier. Rotational levels that are only slightly above the dissociation limit have a substantial centrifugal barrier to dissociation; therefore the tunneling probability is extremely small. However, as rotational excitation further increases, the centrifugal barrier is significantly reduced, and thus the tunneling probability through the centrifugal barrier is dramatically increased.

The photodissociation process, $HOD + h\nu \rightarrow OD + H$, has also been studied at the 121.6 nm.[46] Figure 6 shows the 3D contour of the H-atom product at 121.6 nm excitation. The rotational state distribution shows that the population of the OD($A^2\Sigma^+$) product at $\nu = 0$, $N = 28$, is much larger than that of

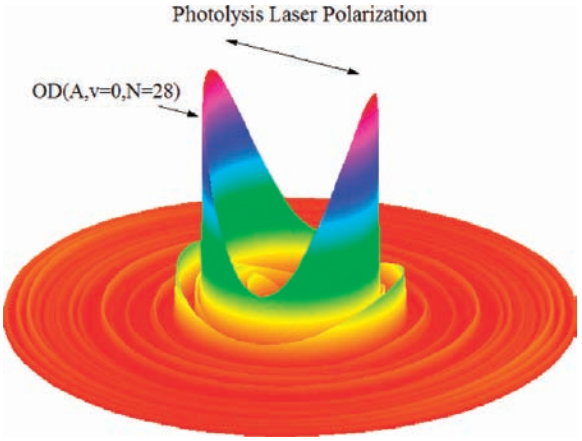

FIGURE 6. The 3D angular dependent translational energy distribution for the HOD + $h\nu$ (121.6 nm) → H + OD (A, v, N), up to an energy of 5000 cm^{-1}. The highest peak is assigned to the OD(A, $v = 0$, $N = 28$) product.

OD in any other rotational states. This is a very interesting and unusual phenomenon. Based on a classical−quantum calculation,[47] this single rotational state product propensity is attributed to a dynamically constrained threshold effect in the HOD photodissociation process.

Recently, van Harrevelt et al.[20] have used their new PESs for water to carry out a complete 3D quantum mechanical description of its photodissociation at a number of energies following $\tilde{B} \leftarrow \tilde{X}$ excitation. Those calculations show that both the absorption spectrum and the product state distributions are strongly influenced by transient resonances on the adiabatic $\tilde{B}$ surface, which probably involve both stretching and bending motions. Excitation of the H_2O to different unstable resonances in the $\tilde{B}$ state using HRTOF has recently been performed in our laboratory.[48] Figure 7 shows 3D plots of the product TE distributions for both OH($X^2\Pi$) and OH($A^2\Sigma^+$) channels from H_2O dissociation via photoexcitation to the five different unstable resonance states on the $\tilde{B}$ state. It is interesting that the rotational distributions of OH($A^2\Sigma^+$) are quite different from those of OH($X^2\Pi$). The distributions of OH($X^2\Pi$) products are closely similar at the five photolysis wavelengths. However, the quantum state distributions and angular distributions of OH($A^2\Sigma^+$) products are dramatically different at five photolysis wavelengths. These features clearly indicate that different unstable resonance excitation on the $\tilde{B}$ state of H_2O has a different effect on the dynamics of OH($X^2\Pi$) and OH($A^2\Sigma^+$) products.

V. H_2O Photochemistry via the $\tilde{C}^1B_1$ Surface: Rotational Dependent Predissociation

The dissociation on the $\tilde{A}$ and $\tilde{B}$ states occurs extremely rapidly, typically in tens of femtoseconds, while the

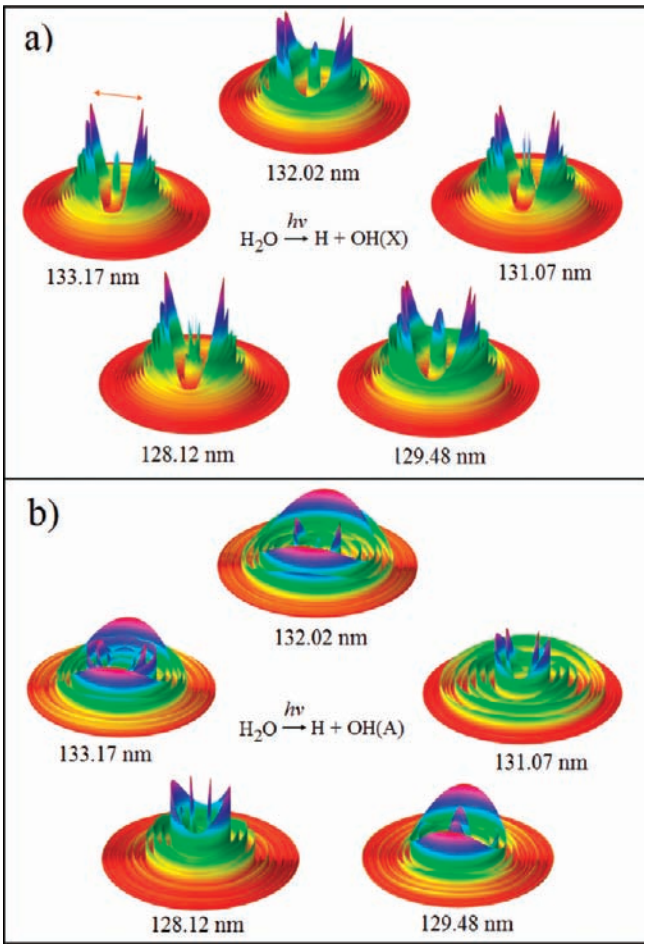

FIGURE 7. The 3D angular dependent product translational energy distributions from H_2O photodissociation through excitation to different unstable periodic orbital states on the $\tilde{B}$ potential energy surface: (a) the H + OH(X) channel; (b) the H + OH(A) channel.

predissociation of the $\tilde{C}^1B_1$ state near 124 nm is much slower. This can be seen by its fully resolved rotational structure. The $\tilde{C}$ state predissociation lifetime is on the order of a few picoseconds. This is much longer than the rotational period of the H_2O molecule, which might result in variable dissociation dynamics. A recent study of the dissociation of H_2O via its $\tilde{C}$ state did indeed reveal rotational-state-specific dissociation dynamics.[49] Figure 8 shows the photodissociation action spectrum for the $\tilde{C} \leftarrow \tilde{X}$ absorption band in which a few rotational lines are clearly resolved. The line widths are rotationally dependent and show an increase that is approximately proportional to $\langle J_a^2 \rangle$ for the excited states. The TOF spectra of the H-atom product for all observed rotational lines were measured. Figure 9 shows the TOF spectra of the H-atom product for two rotational transitions, $0_{00} \leftarrow 1_{10}$ and $1_{10} \leftarrow 0_{00}$. For the $0_{00} \leftarrow 1_{10}$ transition, the two TOF spectra are virtually identical, as is expected for $J' = 0$, which has an isotropic wave function. The OH radicals

produced via this transition are vibrationally excited in the $X^2\Pi$ ground electronic state, with little rotational excitation. The vibrational state distribution for this rotational transition (Figure 10) extends to as high as $v = 13$, with its peak around $v = 7$. No OH products were observed in the $A^2\Sigma^+$ state via this transition. For the $1_{10} \leftarrow 0_{00}$ transition, however, the two TOF spectra for the parallel and perpendicular directions are dramatically different from one another. Most of the OH-($X^2\Pi$) products for this transition are in the $v = 0$ state with extremely high rotational excitation, as are the OH($A^2\Sigma^+$) products.

An explanation for this dramatic variation in the rovibrational product distributions has been given by wavepacket calculations on 3D *ab initio* PESs.[49] Nonadiabatic coupling

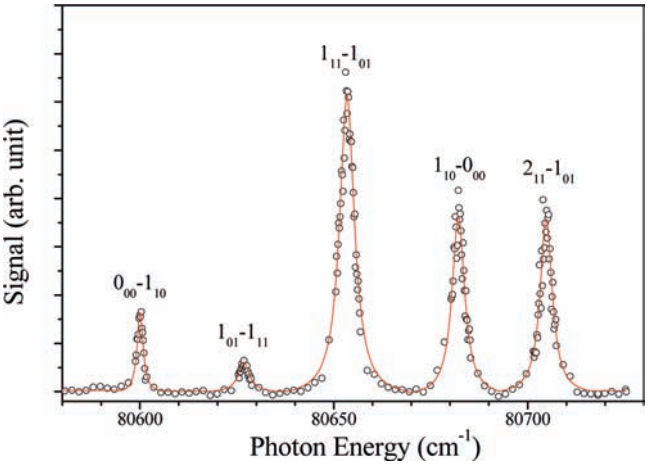

FIGURE 8. The rotational state resolved photodissociation action spectrum of the $\tilde{C}-\tilde{X}$ band.

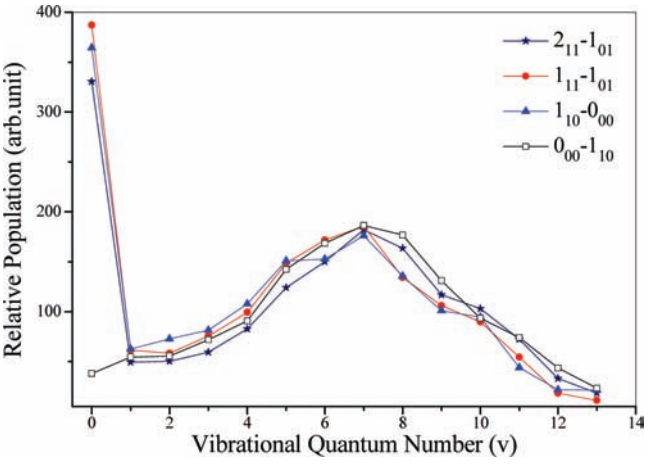

FIGURE 10. The total OH(*X*) vibrational state distribution produced from the different rotational transitions of the $\tilde{C}-\tilde{X}$ band.

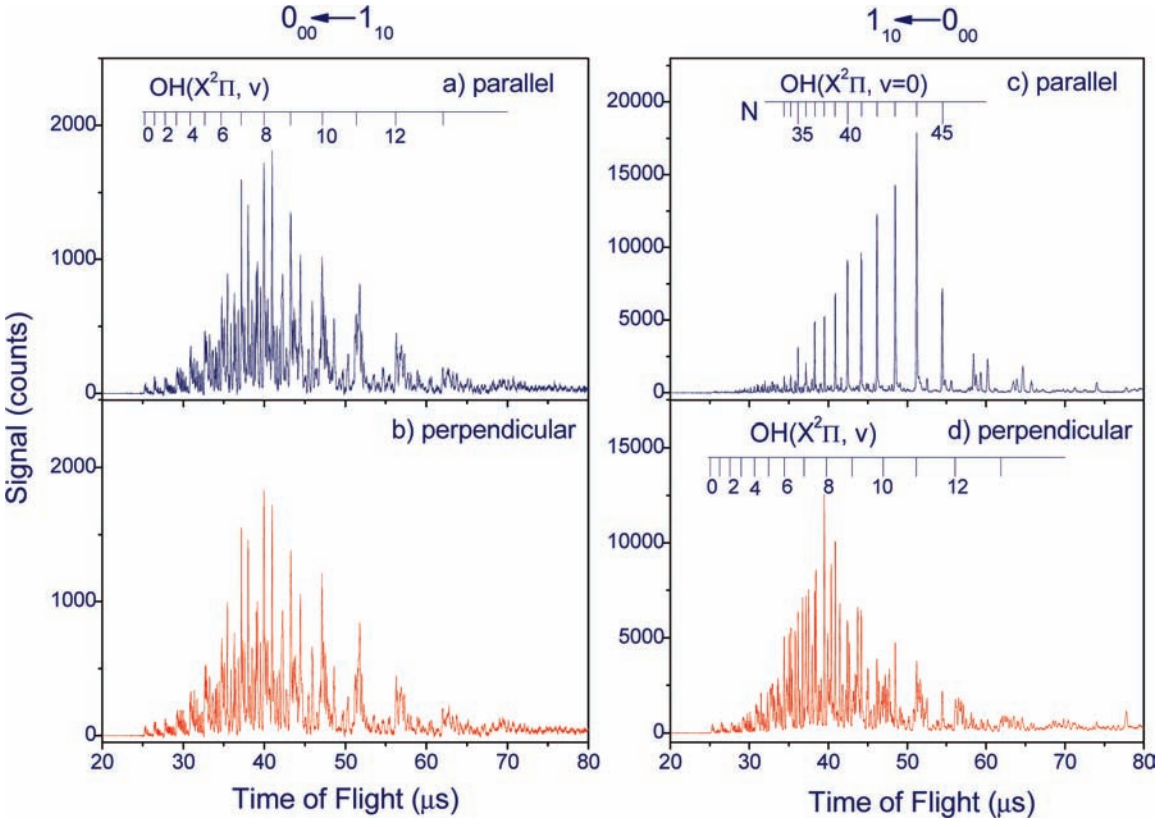

FIGURE 9. Time-of-flight spectra of the H-atom product from H_2O photodissociation via the $0_{00} \leftarrow 1_{10}$ and $1_{10} \leftarrow 0_{00}$ rotational transitions of the $\tilde{C}-\tilde{X}$ band with the detection axis parallel and perpendicular to the laser polarization.

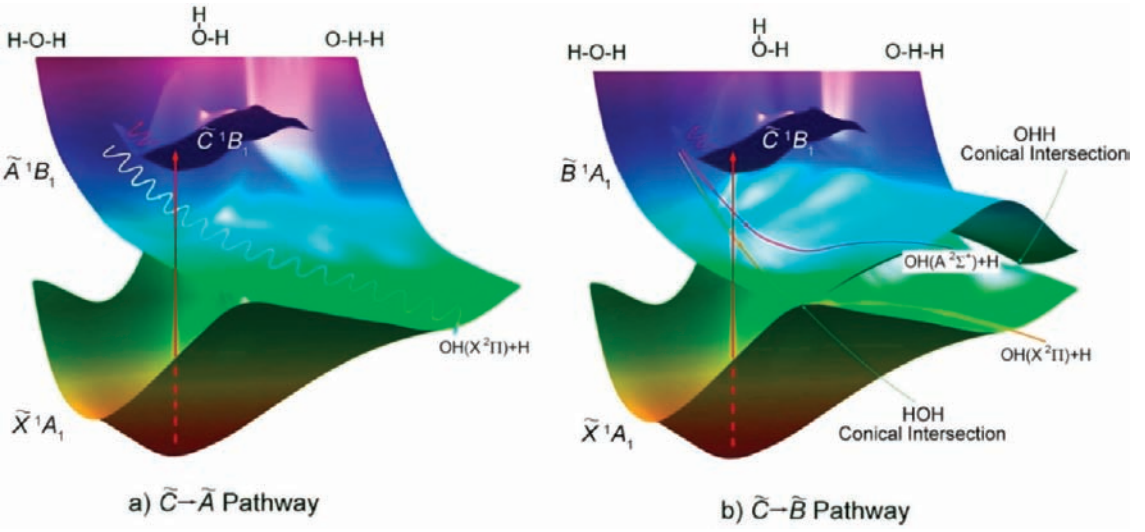

FIGURE 11. The schematics of the two dissociation pathways via the $\tilde{C}$ surface to the $\tilde{B}$ surface and the $\tilde{C}$ surface to the $\tilde{A}$ surface. Clearly, the $\tilde{C} \rightarrow \tilde{B}$ pathway is rotationally mediated. Both product channels, OH ($A^2\Sigma^+$) + H and OH ($X^2\Pi$) + H, can be produced in the $\tilde{C} \rightarrow \tilde{B}$ pathway, while only the OH ($X^2\Pi$) + H channel can be produced in the $\tilde{C} \rightarrow \tilde{A}$ pathway.

between the $\tilde{C}$ state and $\tilde{B}$ state surfaces is mediated by the electronic Coriolis interaction around the *a*-axis of the water molecule, which has a_2 symmetry permitting transfer from $^1B_1$ to $^1A_1$. The dissociation dynamics via this route is quite similar to the direct excitation on the $\tilde{B}$ state. Despite the large vertical energy difference between the $\tilde{C}$ state and $\tilde{A}$ state, the homogeneous coupling route between these two PESs through electronic momentum coupling is still significant. Theoretical analysis shows that the wavepacket on the $\tilde{A}$ surface is completely diverted by the rising potential on the diagonal toward the two low-energy exit valleys, each leading to H + OH($X^2\Pi$). The slalom-like oscillation across these exit valleys is very evident, indicating high vibrational excitation of the OH($X^2\Pi$) products.

Figure 11 illustrates these two dynamically distinctive pathways. The $\tilde{C} \rightarrow \tilde{A}$ pathway is a direct dissociation process through homogeneous coupling that produces vibrationally hot and rotationally cold OH product. The $\tilde{C} \rightarrow \tilde{B}$ pathway proceeds via Coriolis-type coupling that yields extremely rotationally hot and vibrationally cold ground-state OH molecules, as well as rotationally hot OH($A^2\Sigma^+$) molecules. Based on experimental results, the branching ratios between the $\tilde{C} \rightarrow \tilde{A}$ and $\tilde{C} \rightarrow \tilde{B}$ pathways were derived. The branching ratio ($\tilde{C}\rightarrow\tilde{B}/\tilde{C}\rightarrow\tilde{A}$) is dependent on the k_a' quantum number, but more slowly than quadratic, suggesting that there is some rotational enhancement of the $\tilde{C} \rightarrow \tilde{A}$ rate. This remarkable dynamical picture of H_2O photodissociation provides an excellent case of nonadiabatic dynamics involving at least four electronic surfaces.

VI. H_2O Photochemistry via the $\tilde{D}^1A_1$ Surface: Fast Electronic Predissociation through the $\tilde{B}$ State

The absorption band arising from the $\tilde{D}^1A_1$ state with its electronic origin around 122 nm shows no rotational structure. A strong interaction with the $\tilde{B}$ state due to avoiding crossing at bent geometries can explain this feature. The predissociation $\tilde{D} \rightarrow \tilde{B}$ is of purely electronic nature and therefore shows no isotope effect. Two-photon photodissociation dynamics of H_2O via the $\tilde{D}$ state around 122 nm have been investigated recently.[50] The width of the two-photon photodissociation action spectrum of the $\tilde{D} \leftarrow \tilde{X}$ transition gives an estimated lifetime of about 13.5 fs for the state. The OH product TE distributions and angular distributions are qualitatively similar to those of 121.6 nm H_2O photodissociation. This implies that photodissociation of H_2O on the $\tilde{D}$ state proceeds via fast electronically nonadiabatic conversion to the $\tilde{B}$ state and the main dynamical features observed eventually are determined by the topography of the $\tilde{B}$ surface. The similar dynamics between 121.6 and 122 nm suggest that the initial excitation of H_2O at the Lyman-α wavelength might also be through the $\tilde{B} \leftarrow \tilde{X}$ transition rather than the underlying $\tilde{B} \leftarrow \tilde{X}$ continuum. In any case, the dynamics at these two wavelengths are essentially controlled by the $\tilde{B}$ surface. The large discrepancies of branching ratios between experiment and theory suggest that the most recent calculated PESs of H_2O are still inaccurate, especially in describing the nonadiabatic dissociation dynamics.

VII. Concluding Remarks

The photochemistry of the water molecule has been studied using the HRTOF technique in a molecular beam. State-to-state dissociation dynamics have been carefully investigated at different excitation wavelengths. The $\tilde{A}$ state photodissociation of H_2O has been studied at 157.6 nm and was found to be a fast and direct dissociation process on the single PES. The second excited singlet state ($\tilde{B}$) has been investigated at 121.6 nm and between 128 and 133 nm. Direct dissociation on this surface that leads to electronically excited OH($A^2\Sigma^+$) fragments is a minor channel, while the dominant dissociation on this surface that leads to an H-atom plus a rovibrationally excited ground state OH molecule occurs via two conical intersections between $\tilde{B}$ and $\tilde{X}$ states. The strong quantum interference observed from the two dissimilar conical intersection pathways provides a chemical analogue of Young's well-known double-slit experiment. Dissociation on the $\tilde{C}$ state presents an excellent example of rotational dependent predissociation. The $\tilde{C}$ state decays via electronic Coriolis coupling to the $\tilde{B}$ state or through a newly discovered homogeneous nonadiabatic coupling to the $\tilde{A}$ state. Dissociation on the $\tilde{D}$ state has also been studied and shows a fast electronic predissociation to the $\tilde{B}$ state. Through the detailed investigations described above, a clear dynamical picture of H + OH channels from water photochemistry through excitation to its lowest four electronically excited states has been firmly established, providing an excellent case of polyatomic molecular photodissociation. It is necessary to point out that the $O(^1D) + H_2$ channel is not detectable by HRTOF; therefore the importance of this channel is not discussed in this Account. Theoretical evidence in the QCT calculation suggest that this is not a major channel.[43]

We would like to thank our experimental and theoretical collaborators for the research work described in this Account. Financial support from Chinese Academy of Sciences, National Science Foundation of China, and Ministry of Science & Technology of China are greatly appreciated. R.N.D. is supported by the University of Bristol.

BIOGRAPHICAL INFORMATION

Kaijun Yuan was born in 1981 in Hubei, China, and received his B.S. degree in Chemical physics from University of Science and Technique of China (USTC) in 2003. He obtained his Ph.D. degree from the Dalian Institute of Chemical Physics, CAS, in 2008. He is now an assistant research fellow at the State Key Laboratory of Molecular Reaction Dynamics at the Dalian Institute of Chemical Physics. His present research interests are in the area of chemical reaction dynamics in the gas phase.

Richard N. Dixon was born in 1930 in Borough Green, Kent, England, and received his B.Sc. degree in physics from London University in 1951. He received his Ph.D. (1955) and D.Sc. (1976) degrees from Cambridge University. After a spell with the UKAEA, he was a postdoctoral fellow in Canada at the University of Western Ontario (1956−1957) and the National Research Council (1957−1959). He returned to England to a lectureship in chemistry at the University of Sheffield in 1959 and was appointed to a Professorial Chair at the University of Bristol in 1969. He was the Sorby Research Fellow of the Royal Society (1964−1969) and was elected FRS in 1986. He has won many awards, most recently the Rumford Medal of the Royal Society. His main research interests are in molecular spectroscopy, theoretical chemistry, and molecular reaction dynamics.

Xueming Yang was born in 1962 in Zhejiang, China, and received his B.S. degree in physics from Zhejiang Normal University in 1982 and his M. S. degree in chemical physics from Dalian Institute of Chemical Physics, CAS, in 1985. He obtained his Ph.D. in chemistry from University of California at Santa Barbara in 1991. After postdoctoral work at Princeton University and University of California at Berkeley, he became an associated research fellow in the Institute of Atomic and Molecular Sciences in Taipei in 1995 and was promoted to a full research fellow with tenure in 2000. In 2001, he made a move to the Dalian Institute of Chemical Physics, Chinese Academy of Sciences, and became the director of the State Key Laboratory of Molecular Reaction Dynamics. His main research interests are in the area of experimental chemical dynamics in the gas phase and at interfaces.

FOOTNOTES

*To whom correspondence should be addressed. E-mail: xmyang@dicp.ac.cn.

REFERENCES

1 Kukura, P.; McCamant, D. W.; Yoon, S.; Wandschneider, D. B.; Mathies, R. A. Structural observation of the primary isomerization in vision with femtosecond -stimulated Raman. *Science* **2005**, *310*, 1006–1009.

2 Bonev, B. P.; Mumma, M. J. A comprehensive study of infrared OH prompt emission in two comets. Implications for unimolecular dissociation of H_2O. *Astrophys. J.* **2006**, *653*, 788–791.

3 Yoshino, K.; Esmond, J. R.; Parkinson, W. H.; Ito, K.; Matsui, T. Absorption cross section measurements of water vapor in the wavelength region 120 to 188 nm. *Chem. Phys.* **1996**, *211*, 387–391.

4 Hennig, S.; Engel, V.; Schinke, R.; Staemmler, V. Emission spectroscopy of photodissociating water molecules. A time-independent ab-initio study. *Chem. Phys. Lett.* **1988**, *149*, 455–462.

5 Kuhl, K.; Schinke, R. Time-dependent rotational state distributions in direct photodissociation. *Chem. Phys. Lett.* **1989**, *158*, 81–86.

6 Schinke, R.; Engel, V.; Staemmler, V. Ab-initio study of the photodissociation of water. OH state distributions and comparison with experiment. *Chem. Phys.Lett.* **1985**, *116*, 165–168.

7 Zhang, J. Z.; Imre, D. G. Spectroscopy and photodissociation dynamics of H_2O. Time-dependent view. *J. Chem. Phys.* **1989**, *90*, 1666–1676.

8 Andresen, P.; Beushausen, V.; Hausler, D.; Lulf, H. W.; Rothe, E. W. Strong propensity rules in the photodissociation of a single rotational quantum state of vibrationally excited H_2O. *J. Chem. Phys.* **1985**, *83*, 1429–1430.

9 Hausler, D.; Andresen, P.; Schinke, R. State to state photodissociation of H_2O in the 1st absorption-band. *J. Chem. Phys.* **1987**, *87*, 3949–3965.

10 Schinke, R.; Vanderwal, R. L.; Scott, J. L.; Crim, F. F. The effect of bending vibrations on product rotations in the fully state-resolved photodissociation of the A-state of water. *J. Chem. Phys.* **1991**, *94*, 283–288.

11 Engel, V.; Staemmler, V.; Vanderwal, R. L.; Crim, F. F.; Sension, R. J.; Hudson, B.; Andresen, P.; Hennig, S.; Weide, K.; Schinke, R. Photodissociation of water in the 1st

absorption-band. A prototype for dissociation on a repulsive potential-energy surface. *J. Phys. Chem.* **1992**, *96*, 3201–3213.

12 Brouard, M.; Langford, S. R.; Manolopoulos, D. E. New trends in the state-to- state photodissociation dynamics of H_2O(A). *J. Chem. Phys.* **1994**, *101*, 7458–7467.

13 Grunewald, A. U.; Gericke, K. H.; Comes, F. J. Photodissociation of room- temperature and jet-cooled water at 193 nm. *Chem. Phys. Lett.* **1987**, *133*, 501–506.

14 Guo, H.; Murrell, J. N. Dynamics of the A-state photodissociation of H_2O at 193 nm. *Mol. Phys.* **1988**, *65*, 821–827.

15 Engel, V.; Schinke, R.; Staemmler, V. Photodissociation dynamics of H_2O and D_2O in the 1st absorption-band. A complete ab-initio treatment. *J. Chem. Phys.* **1988**, *88*, 129–148.

16 Andresen, P.; Ondrey, G. S.; Titze, B.; Rothe, E. W. Nuclear and electron dynamics in the photodissociation of water. *J. Chem. Phys.* **1984**, *80*, 2548–2569.

17 Mikulecky, K.; Gericke, K. H.; Comes, F. J. Decay dynamics of $H_2O(^1B_1)$. Full characterization of OH product state distribution. *Chem. Phys. Lett.* **1991**, *182*, 290–296.

18 Weide, K.; Schinke, R. Photodissociation dynamics of water in the second absorption band II. Ab-initio calculation of the absorption spectra for water and water-d_2 and dynamical interpretation of diffuse vibrational structures. *J. Chem. Phys.* **1989**, *90*, 7150–7163.

19 Dricke, M.; Heumann, B.; Kuhl, K.; Schroder, T.; Schinke, R. Fluctuation in absorption spectra and final product state distributions following photodissociation process. *J. Chem. Phys.* **1994**, *101*, 2051–2068.

20 Harrevelt, R.; Hemert, M. C. Photodissociation of water II. Wave-packet calculations for the photofragmentation of H_2O and D_2O in the B band. *J. Chem. Phys.* **2000**, *112*, 5787–5808.

21 Weide, K.; Kuhl, K.; Schinke, R. Unstable periodic orbits, recurrences, and diffuse vibrational strucutres in the photodissociation of water near 128nm. *J. Chem. Phys.* **1989**, *91*, 3999–4008.

22 Dixon, R. N.; Hwang, D. W.; Yang, X. F.; Harich, S.; Lin, J. J.; Yang, X. Chemical "double slits": Dynamical interference of photodissociation pathways in water. *Science* **1999**, *285*, 1249–1253.

23 Segev, E.; Shapiro, M. Three-dimensional quantum dynamics of H_2O and HOD photodissociation. *J. Chem. Phys.* **1982**, *77*, 5604–5623.

24 Weide, K.; Schinke, R. Photodissociation dynamics of water in the 2nd absorption-band . Rotational state distributions of $OH(^2\Sigma)$ and $OH(^2\Pi)$. *J. Chem. Phys.* **1987**, *87*, 4627–4633.

25 Dixon, R. N. The Role of inter-state renner-teller coupling in the dissociation of triatomic-molecules. A time-dependent approach. *Mol. Phys.* **1985**, *54*, 333–350.

26 Krautwald, H. J.; Schnieder, L.; Welge, K. H.; Ashfold, M. N. R. Hydrogen-atom photofragment spectroscopy. Photodissociation dynamics of H_2O in the B-X absorption-band. *Faraday Discuss.* **1986**, *82*, 99–110.

27 Fillion, J. H.; van Harrevelt, R.; Ruiz, J.; Castillejo, N.; Zanganeh, A. H.; Lemaire, J. L.; van Hemert, M. C.; Rostas, F. Photodissociation of H_2O and D_2O in $\tilde{B}$, $\tilde{C}$, and $\tilde{D}$ states (134−119 nm). Comparison between experiment and ab-initio calculations. *J. Phys. Chem. A* **2001**, *105*, 11414–11424.

28 Zanganeh, A. H.; Fillion, J. H.; Ruiz, J.; Castillejo, M.; Lemaire, J. L.; Shafizadeh, N.; Rostas, F. Photodissociation of H_2O and D_2O below 132 nm. *J. Chem. Phys.* **2000**, *112*, 5660–5671.

29 Schatz, G. C. A coupled states distorted-wave study of the $O(^3P) + H_2$ (D_2, HD, DH) reaction. *J. Chem. Phys.* **1985**, *83*, 5677–5686.

30 Mordaunt, D. H.; Ashfold, M. N. R.; Dixon, R. N. Dissociation dynamics of $H_2O(D_2O)$ following photoexcitation at the Lyman-α Wavelength (121.6 nm). *J. Chem. Phys.* **1994**, *100*, 7360–7375.

31 Ashfold, M. N. R.; Bayley, J. M.; Dixon, R. N. The $4s^1b_1$ and $3d^1b_1$ Rydberg states of H_2O and D_2O. Spectroscopy and predissociation dynamics. *Can. J. Phys.* **1984**, *62*, 1806–1833.

32 Kuge, H. H.; Kleinermanns, K. Rotational predissociation of H_2O (C^1B_1) studied by multiphoton ionization spectroscopy in a supersonic free-jet. *J. Chem. Phys.* **1989**, *90*, 46–52.

33 Hodgson, A.; Simons, J. P.; Ashfold, M. N. R.; Bayley, J. M.; Dixon, R. N. Quantum state-selected photodissociation dynamics in H_2O and D_2O. *Mol. Phys.* **1985**, *54*, 351–368.

34 Ashfold, M. N. R.; Bayley, J. M.; Dixon, R. N. Molecular predissociation dynamics revealed through multiphoton ionization spectroscopy. The C^1B_1 states of H_2O and D_2O. *Chem. Phys.* **1984**, *84*, 35–50.

35 van Harrevelt, R.; van Hemert, M. C. Photodissociation of water. I. Electronic structure calculations for the excited states. *J. Chem. Phys.* **2000**, *112*, 5777–5786.

36 Schnieder, L.; Meier, W.; Welge, K. H.; Ashfold, M. N. R.; Western, C. M. Photodissociation dynamics of H_2S at 121.6 nm and a determination of the potential-energy function of $SH(A^2\Sigma^+)$. *J. Chem. Phys.* **1990**, *92*, 7027–7037.

37 Yuan, K. J.; Cheng, L. N.; Cheng, Y.; Guo, Q.; Dai, D. X.; Yang, X. M. Tunable VUV photochemistry using Rydberg H-atom time-of-flight spectroscopy. *Rev. Sci. Instrum.* **2008**, *79*, No. 124101.

38 Hwang, D. W.; Yang, X. F.; Harich, S.; Lin, J. J.; Yang, X. M. Photodissociation dynamics of H_2O at 121.6 nm: Effect of parent rotational excitation on reaction pathways. *J. Chem . Phys.* **1999**, *110*, 4123–4126.

39 Hwang, D. W.; Yang, X. F.; Yang, X. M. The vibrational distribution of the OH product from H_2O photodissociation at 157 nm: Discrepancies between theory and experiment. *J. Chem . Phys.* **1999**, *110*, 4119–4122.

40 Yang, X. F.; Hwang, D. W.; Lin, J. J.; Ying, X. M. Dissociation dynamics of the water molecule on the A^1B_1 electronic surface. *J. Chem. Phys.* **2000**, *113*, 10597–10604.

41 Lu, I. C.; Wang, F. Y.; Yuan, K. J.; Cheng, Y.; Yang, X. M. Nonstatistical spin dynamics in photodissociation of H_2O at 157 nm. *J. Chem. Phys.* **2008**, *128*, 066101.

42 van Harrevelt, R.; van Hemert, M. C. Photodissociation of water in the A band revisited with new potential-energy surfaces. *J. Chem. Phys.* **2001**, *114*, 9453–9462.

43 Harich, S. A.; Hwang, D. W. H.; Yang, X. F.; Lin, J. J.; Yang, X. M.; Dixon, R. N. Photodissociation of H_2O at 121.6 nm: A state-to-state dynamical picture. *J. Chem. Phys.* **2000**, *113*, 10073–10090.

44 Guo, H. The B-state photodissociation of water. A classical trajectory study. *Mol. Phys.* **1989**, *68*, 249–254.

45 Harich, S. A.; Yang, Y. F.; Yang, X. M. Extremely rotationally excited OH from water (HOD) photodissociation through conical intersection. *Phys. Rev. Lett.* **2001**, *87*, No. 253201.

46 Harich, S. A.; Yang, X. F.; Yang, X.; van Harrevelt, R.; van Hemert, M. C. Single rotational product propensity in the photodissociation of HOD. *Phys. Rev. Lett.* **2001**, *87*, No. 263001.

47 van Harrevelt, R.; van Hemert, M. C.; Schatz, G. C. A comparative classical- quantum study of the photodissociation of water in the B band. *J. Phys. Chem. A* **2001**, *105*, 11480–11487.

48 Cheng, Y.; Yuan, K. J.; Cheng, L.; Guo, Q.; Dai, D. X.; Yang, X. M. Photodissociation dynamics of H_2O: Effect of unstable resonances on the $\tilde{B}(^1A_1)$ electronic state. *J. Chem. Phys.* **2011**, x.

49 Yuan, K. J.; Cheng, Y.; Cheng, L.; Guo, Q.; Dai, D. X.; Wang, X. Y.; Yang, X. M.; Dixon, R. N. Nonadiabatic dissociation dynamics in H_2O: Competition between rotationally and non-rotationally mediated pathways. *Proc. Natl. Acad. Sci. U.S.A.* **2008**, *105*, 19148–19153.

50 Yuan, K. J.; Cheng, L. N.; Cheng, Y.; Guo, Q.; Dai, D. X.; Yang, X. M. Two-photon photodissociation dynamics of H_2O via the $\tilde{D}$ state. *J. Chem. Phys.* **2009**, *131*, No. 074301.